# Integrated 3-D Printable Temperature Sensor for Advanced Manufacturing

**Nuwan Munasinghe and Gavin Paul**
University of Technology Sydney, Australia
{Nuwan.Munasinghe, Gavin.Paul}@uts.edu.au

## Abstract

As technology continues to develop at a rapid pace, the world progresses towards the fourth industrial revolution, Industry 4.0, with advancements in automation and machine intelligence, as well as manufacturing breakthroughs leading to more efficient and advanced methods. Additive manufacturing (AM), also known as 3D printing, is a type of manufacturing method that has experienced great development and has revolutionised end-product manufacturing. The authors are involved in a project to develop a large-scale industrial 3D printer to print equipment called a Gravity Separation Spiral (GSS), and in an effort to make the equipment "smart", sensors need to be embedded inside to monitor the operating conditions remotely. This paper presents a temperature sensor able to be printed by a multi-material 3D printer, into 3D printed equipment. In this method, a conductive carbon-based filament has been used to print temperature-sensitive traces inside a Polylactic Acid (PLA) base. The printed sensor was temperature tested in a controlled environment using a programmable heat pad, and the change in resistance has been measured as a voltage change using a data acquisition device. Tests were conducted within in the expected operating range, between 25 ℃ and 36 ℃, and the absolute temperature error was found to be less than ±2 ℃.

## 1 Introduction

Additive manufacturing (AM), widely known as 3D printing, is the process of manufacturing objects using a computer designed model. The advantages of this method include a reduction in material wastage, and the ability to customise the design, allowing the user to produce complex and intricate shapes with high precision, thus, providing the ability to potentially manufacture new devices that may not be possible using traditional manufacturing methods. Although there is a significant amount of initial capital involved, it is predicted that the cost of employing these technologies will likely reduce in the next few years, and the cost saved can be as high as 70% by reducing the requirement for tooling [CSRIO, 2016]. Since AM is transforming from a prototyping technology to an end-product manufacturing technique [Wong and Hernandez, 2012], different industries such as construction, aviation and medicine are integrating this technology into their applications [Tadjdeh, 2014; Shakor *et al.*, 2019; Cheng *et al.*, 2017].

The authors are working with UTS Rapido on a project to develop a 3D printer to print a Gravity Separation Spiral (GSS), a machine that is used around the world to separate minerals from the slurry. This new manufacturing method will allow for greater customisation compared to traditional mould-based manufacturing, and will provide economic benefits. Apart from developing a 3D printer, the team is also working on researching and developing sensors that can be embedded, or printed inline during the manufacturing process. A GSS with embedded internet of things (IoT) sensors will enable remote monitoring of its operation conditions, as well as various parameters such as wear, strain, and flow rate [Munasinghe *et al.*, 2019a; Munasinghe *et al.*, 2019b; Munasinghe *et al.*, 2021; Munasinghe and Paul, 2019; Munasinghe and Paul, 2020c; Munasinghe and Paul, 2020b; Munasinghe and Paul, 2020a]. 3D printed sensors provide advantages such as low cost and highly customisable shapes that can enable seamless integration with the structure without compromising its overall mechanical properties [Georgousis *et al.*, 2015].

Embedded temperature sensors have been used in various industrial applications to monitor the state of equipment. IoT based temperature monitoring systems embedded in CNC machines have been developed to monitor machine process [Al-Saedi *et al.*, 2017]. Embedded thermal monitoring sensors, based on fibre-optic sensors for electrical coils to determine its operational integrity, have been developed by Mohammad et al [Mohammad and Djurovic, 2016]. Thermocouples have been directly fabricated onto turbine engine components providing improved reliability, robustness and serviceability in harsh environments [Gutleber *et al.*, 2006].

A 3D printed hydrogel-based temperature sensor was developed by Lei et al [Lei *et al.*, 2017], featuring a submillimetre resolution skin-like sensor. This sensor works on the principle of capacitance change when hydrogel fibres are subjected to different temperatures. This temperature sensor can measure temperatures between 25 ℃ and 50 ℃. In addition to measuring the temperature, this sensor can also evaluate pressure and touch as well. This technology can be applied in personal healthcare products such as watches and other wearable devices, and can also be applied in soft robotics applications as it is highly compliant.

3D direct laser writing has been used to create micrometre sized local temperature sensors that can be placed lithographically. This method has been used by Wickberg et al. [Wickberg *et al.*, 2015] to place temperature sensors onto an electronic chip. In a test where the sensor had to record data in 1 second increments, it displayed an accuracy of 0.5 K. This type of sensor is useful for fast and accurate local temperature detection, as well as when a micrometre spatial resolution is required.

Microfluidic and liquid metals have been used to 3D print an inverted-F antenna where the temperature measured was dependent on the resonant frequency [Wang *et al.*, 2019]. With the change in temperature, thermal volume expansion occurs and the antenna length changes, effectively altering its resonant frequency. An increasing temperature results in a decrease in resonant frequency, and a near-linear relationship between these two factors has been observed. Simulated results showed the sensitivity of the temperature being 2.54 MHz/℃. Another wireless passive temperature sensor based on microfluidic and liquid metal technologies has been developed by Traille et al. [Traille *et al.*, 2011]. In this method, liquid metal has been used to alter the number of antennas dynamically along with a linear array arrangement with respect to the temperature. The temperature-expansion of liquid metal short-circuits a number of gaps inside, bridging the microfluidic gaps together, resulting to a change in the radar cross-section. This sensor has a tunable temperature of at least 20 K and a resolution of around 4 K.

Inkjet printing of silver nanoparticles has been used to design a resistance-based temperature and humidity sensor by Courbat et al [Courbat *et al.*, 2011]. Temperature and humidity affect the electrical properties of printed silver structures on paper. The printed temperature sensor was tested between -20 ℃ and 60 ℃ and observed a near-linear relationship between resistance and temperature. They observed the temperature coefficient of resistance (TCR) value of 0.0011 ℃$^{-1}$ during the experiments. Measurements of the humidity depends on the capacitance change in silver traces and showed an exponential response to the humidity level.

Conductive paint made from latex and exfoliated graphite has also been used to develop temperature sensors to measure temperature over an area [Sauerbrunn *et al.*, 2015]. This approach is amenable for additive manufacturing technologies. The paint was spray-coated over a stencilled area in multiple layers. Tests were conducted between 20 ℃ and 60 ℃ and observed TCR between -0.75x10$^{-1}$℃$^{-1}$ and -0.97x10$^{-1}$℃$^{-1}$. In this method, it has been observed that an increase in temperature results in a negative TCR, hence exhibiting two opposing effects - thermal expansion causing a decrease in percolation through the composite, thus resulting in increased resistance, and an increase in conductivity of the carbon particles, which have negative TCR. In this case, with 30% exfoliated graphite (EG), the dominant factor was the reduction in percolation due to thermal expansion of the polymer.

Printable nanocomposite ink has been used by Harada et al. [Harada *et al.*, 2014] to print temperature sensors as well as strain sensors. These temperature and strain sensors are printed on a flexible substrate and are shaped as animal whiskers, imitating its ability to detect spatial distribution (using strain) and animal skin (using temperature). According to their results, the sensor was tested between 25.8 ℃ and 53.2 ℃, with a sensitivity of approximately 0.63%℃$^{-1}$. Additionally, the mechanical and electrical reliabilities of the sensor were characterised to confirm if bending the substrate has any effect on the sensor. This sensor can be used in robotics to get information about the environment and in artificial skins.

In this research, carbon-based material has been used to print the temperature sensor. The main reason for this is due to its positive-temperature-coefficient (PTC), and according to Zhang et al. [Zhang *et al.*, 2014], these composites exhibited little to no change in its PTC value despite undergoing multiple heating cycles. Other advantages are its low cost and its abundance, hence making it suitable for mass manufacturing. In addition, this material is corrosion resistant, which is a valuable factor for sensors. In this project, other wear and strain sensors have been developed using the same material, thus reducing the production complexity [Munasinghe *et al.*, 2019a; Munasinghe *et al.*, 2019b].

The rest of this paper is organised as follows: Section 2 explains the methodology behind the sensor; Section 3 presents experimental results; Section 4 discusses the results, and finally, Section 5 presents the conclusions.

## 2 Methodology

### 2.1 Principle of Temperature Sensors

Temperature measurement is often based on relative changes of various physical properties, such as electrical resistance and volume, in addition to the change in temperature itself. In general, this relationship can be expressed by (1), the property, $R$, the temperature change, $dT$ and the temperature coefficient $\alpha$. In this experiment, $R$, is the electrical resistance in the 3D printed traces. By assuming $\alpha$ does not change significantly with the temperature, a linear approximation can be used to estimate the value of $R_T$ in a given temperature, $T$; and the reference value of the property, $R_0$ at a reference temperature $T_0$. Eq. (2) shows this relationship. But this method only works if the $R$ changes with the temperature linearly. In this experiment, we observed that for 3D printed conductive traces, the relationship between $R$ and $T$ is not purely linear. Therefore, a non-linear approximation method has been used as shown in (3) to fit a polynomial of degree 2 for the testing temperature range, where $A, B$ and $C$ are constants valid for the tested temperature range.

$$dR/R = \alpha \cdot dT \tag{1}$$

$$R_T = R_{T_0}(1 + \alpha(T - T_0)) \tag{2}$$

$$R = AT^2 + BT + C \tag{3}$$

### 2.2 Resistance Measurement

The 3D printed sensor's resistance will change as the temperature changes. Hence, it is imperative to accurately measure this parameter to monitor minute changes. To do that, the Wheatstone bridge-based approach has been used. In this method, $\Delta V$ can be measured relative to the resistance of the temperature sensor. To measure the voltage accurately, a data acquisition device (DAQ) has been used. The arrangement of different bridge components are shown in Fig. 3a; the relationship between the sensor resistance, $R_T$, other bridge resistance values, $(R_1, R_2, R_3)$, input voltage, $E$ and measured voltage, $\Delta V$ are shown in (4).

$$\Delta V = E \cdot \left( \frac{R_2}{R_2 + R_3} - \frac{R_T}{R_1 + R_T} \right) \tag{4}$$

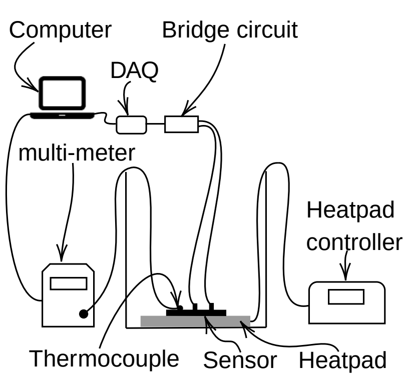


Figure 1: Experiment setup.

Table 1: Sensor dimensions

| Dimension | Value (mm) |
|---|---|
| Trace width | 1 |
| Trace height | 1 |
| Trace length | 1041.14 |
| Terminal inner diameter | 3 |
| Terminal outer diameter | 5 |
| Terminal height | 4.5 |
| Total radious (r) | 30.6 |

## 3 Experiment Results

### 3.1 Design of the Sensor

The overall shape of the sensor is circular and there are traces starting from the centre of the sensor that run in a concentric spiral pattern, outwards. There are two terminals - one in the middle, and one at the outside as shown in Fig. 3b. An image of a 3D view of the sensor and the printed sensor are shown in Fig. 3c and Fig. 3d, respectively. The dimensions of the sensor are shown in Table 1.

### 3.2 Material and Printing Process

Conductive carbon traces were printed with Proto-pasta conductive Polylactic Acid (PLA) filament. This material is made with a mixture of PLA and carbon black. The resistivity of this filament was rated at 15 Ω.cm before printing. After printing, this increased to 30 Ω.cm along the X-Y plane, and 115 Ω.cm along the Z-axis. The sensor was printed by the Prusa i3 MK3 with the Multi-Material Unit 2.0 attachment. This printer is a material extrusion printer [ISO;ASTM, 2015] which extrudes melted material through a nozzle, and the added

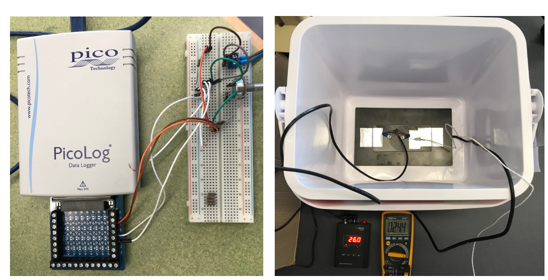


(a) (b)

Figure 2: a) DAQ and the bridge circuit. b) Sensor inside a box with a data logging multi-meter.

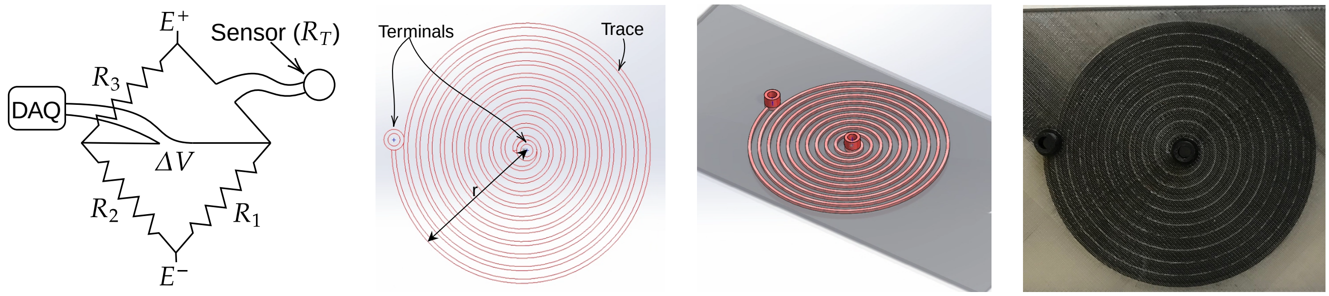


Figure 3: a) Wheatstone bridge setup. b) Wire-frame view of the sensor. c) 3D view of the sensor. d) Printed sensor.

attachment provides the ability to load 5 filaments simultaneously, making it capable of creating objects composed of different materials in a single print. The sensor was printed with a nozzle temperature of 210 ℃ for PLA and 240 ℃ for conductive filament.

### 3.3 Experiment Setup

As mentioned in Section 2, in this experiment, a DAQ (PicoLog 1000 series data logger) has been used. This DAQ has been used to apply a constant voltage (5 V) to the bridge circuit and then to collect and log data to a computer. To set the resistance exactly with the sensor and balance the bridge, a variable resistor has been used, shown in Fig. 2a. To maintain a constant surface temperature with fewer effects from the wind, the sensor was placed inside a box (Fig. 2b). A data logging multimeter was used to measure the temperature of the sensor using a thermocouple, which then wirelessly logged the data to a computer. Fig. 1 shows the wireless connection as an unbroken line to the computer to illustrate the strong connection. The sensor was placed on a temperature controllable heat pad (RDK) where a thermocouple has been connected to the top of the sensor using a metallic tape. The heat pad has buttons to set the required temperature and a digital screen to display the current temperature. Additionally, the sensor was taped onto the heat pad using metallic tape to allow for good thermal contact. The complete experimental setup is shown in Fig. 1.

### 3.4 Sensor Calibration

Five calibration tests were conducted for the initial calibration of the printed sensor, where the voltage change $\Delta V$ and the temperature were recorded. The temperature of the heat pad was at room temperature (24-26 ℃). Before starting to collect data, the heat pad temperature was set to a constant value (38 ℃). This upper bound temperature was chosen because at 42 ℃, PLA starts to deform. Therefore, a temperature slightly lower than when this deformation begins has been selected. At the start of the test, the heat pad was turned on and the temperature and voltage data were logged simultaneously until the heat pad reached the preset temperature. This was considered as a single test, where afterwards the system was then provided time to cool back down to room temperature. By plotting the $\Delta V$ vs temperature, it was evident that a polynomial of degree 2 was the best fit for the relationship. Hence, a polynomial of degree 2 was fitted to the data and constant values were identified ($A = 0.0002, B = -0.0051, C = -0.0016$) as per (3). These test results are shown in Fig. 4.

### 3.5 Testing the Sensor After Calibration

After identifying the characteristics of the sensor, it was then tested by measuring the voltage and predicting the temperature using the fitted polynomial. This test was conducted in the same way as before with the heat pad, which was done by measuring the temperature and voltage using the DAQ. The results of different test cases and predicted temperature using the polynomial are shown in Fig. 5. Additionally, for each test, another graph (Fig. 6) was plotted to visualise the absolute error values. According to Fig. 6, it can be seen that the maximum absolute error that was able to be measured using the 3D printed temperature sensor was less than ±2 ℃.

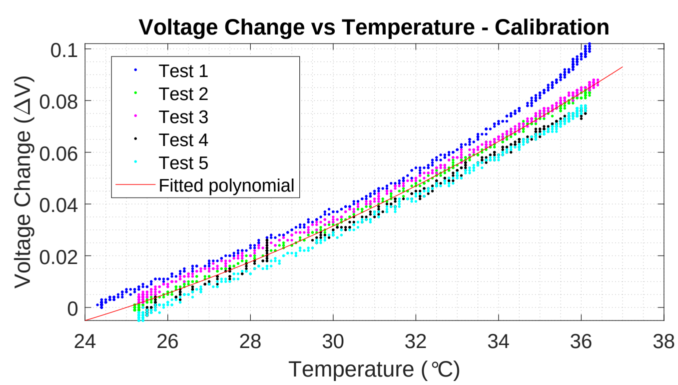


Figure 4: Calibration test results.

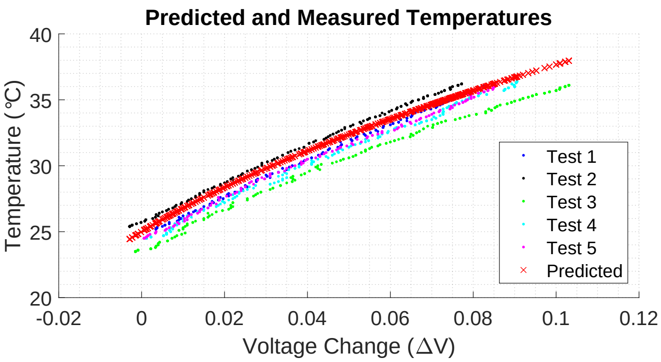


Figure 5: Temperature prediction test results.

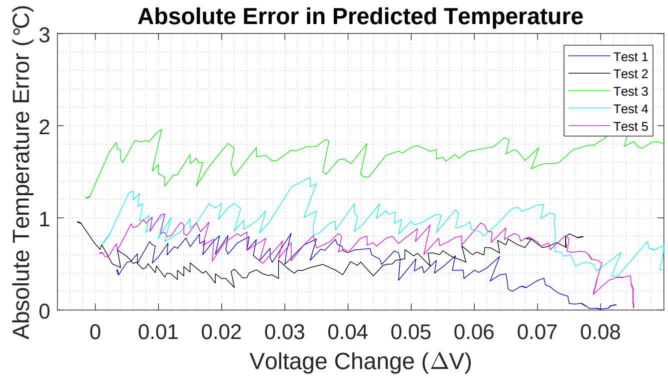


Figure 6: Absolute error.

## 4 Discussion

From the results, it can be seen that the proposed methodology to print a temperature sensor using carbon-based conductive filament and a Wheatstone-bridge based voltage measurement provides accurate results with an error margin of ±2 ℃ which is less than the required error margin of ±5 ℃ for this application. The results show that the relationship between the temperature and the voltage of this selected material is relatively linear, but to improve the accuracy, a polynomial of degree 2 has been used. The proposed method uses inexpensive carbon-based conductive filament to print the temperature sensor and the printed sensor was embedded in a PLA base. However, this kind of 3D printed sensor can be embedded in any kind of 3D printed object with similar material to measure its internal temperature. A notable advantage of printed sensors over conventional temperature sensors placed in sockets is the ability to print them inline with the object, eliminating post-processing involved to measure its conditions. Additionally, providing space for conventional sensors might affect structural integrity due to the sensor being made with different materials compared to the object. This becomes a significant concern if the sensor needs to be placed deep inside the material. On the other hand, the advantage of placing conventional sensors is that it does not require calibration like 3D printed sensors since the sensors are already calibrated by the manufacturer therefore easy to integrate. Additionally, separate research is underway to test the long-term creep and long-term weathering effect on the material. The sensor in this paper was manufactured using an extrusion-based printing method, which is a commercially available, commonly utilised, and inexpensive printing method. A similar technique has also been used by the authors to print wear and strain sensors. The temperature sensor developed in this research can also augment the authors' previous developed sensors, such as by investigating a more accurate temperature-compensated strain sensor [Munasinghe *et al.*, 2019a; Munasinghe *et al.*, 2019b].

## 5 Conclusion

In conclusion, this research proposed a 3D printable temperature sensor which can be embedded into 3D printed equipment or objects to measure its conditions remotely. The proposed method uses carbon-based PLA to print a circular temperature sensor which is embedded inside a PLA base. Results show that the proposed sensor yields results within an acceptable error margin. This method will reduce the complexity of trying to embed conventional sensors inside 3D printed objects and reduce the manufacturing complexity by removing the post-processing operation. The proposed method uses inexpensive material and utilises a commonly used printing method, and is expected to complement research on other 3D printed sensors.

## Acknowledgements

This research is supported by UTS, The Commonwealth of Australia's Department of Industry, Innovation and Science (Innovative Manufacturing CRC Ltd) and Downer, via its subsidiary Mineral Technologies. Thank you to Rapido, in particular, Hervé Harvard and Michael Behrens for establishing this overall research activity and leading the overall R&D engineering project. Authors thank Lewis Miles, for helping with designing and printing the sensor. We also thank UTS:RI/CAS for providing required resources to carry out this research.

## References

[Al-Saedi *et al.*, 2017] Ibtesam R. K. Al-Saedi, Farag Mahel Mohammed, and Saifaldeen S Obayes. CNC machine based on embedded wireless and Internet of Things for workshop development. In *Int. Conf. on Control, Automation and Diagnosis*, pages 439–444. IEEE, 1 2017.

[Cheng *et al.*, 2017] George Z Cheng, Erik Folch, Adam Wilson, Robert Brik, Noah Garcia, Raul San Jose Estepar, Jorge Onieva Onieva, Sidhu Gangadharan, and Adnan Majid. 3D Printing and Personalized Airway Stents. *Pulmonary Therapy*, 3(1):59–66, 2017.

[Courbat *et al.*, 2011] J. Courbat, Y.B. Kim, D. Briand, and N.F. de Rooij. Inkjet printing on paper for the realization of humidity and temperature sensors. In *Int. Solid-State Sensors, Actuators and Microsystems Conference*, pages 1356–1359. IEEE, 6 2011.

[CSRIO, 2016] CSRIO. Advanced manufacturing : A Roadmap for unlocking future growth opporunities for Australia. Technical Report November, 2016.

[Georgousis *et al.*, 2015] G Georgousis, C Pandis, A Kalamiotis, P Georgiopoulos, A Kyritsis, E Kontou, P Pissis, M Micusik, K Czanikova, J Kulicek, and M Omastova. Strain sensing in polymer/carbon nanotube composites by electrical resistance measurement. *Composites Part B: Engineering*, 68:162–169, 2015.

[Gutleber *et al.*, 2006] Jonathan Gutleber, Jeffrey Brogan, R.J. Gambino, Christopher Gouldstone, Robert Greenlaw, Sanjay Sampath, Jon Longtin, and Dongming Zhu. Embedded Temperature and Heat Flux Sensors for Advanced Health Monitoring of Turbine Engine Components. In *IEEE Aerospace Conference*, volume 2006, pages 1–9, 2006.

[Harada *et al.*, 2014] Shingo Harada, Wataru Honda, Takayuki Arie, Seiji Akita, and Kuniharu Takei. Fully Printed, Highly Sensitive Multifunctional Artificial Electronic Whisker Arrays Integrated with Strain and Temperature Sensors. *ACS Nano*, 8(4):3921–3927, 4 2014.

[ISO;ASTM, 2015] ISO;ASTM. Standard Terminology for Additive Manufacturing – General Principles – Terminology. Technical report, 2015.

[Lei *et al.*, 2017] Zhouyue Lei, Quankang Wang, and Peiyi Wu. A multifunctional skin-like sensor based on a 3D printed thermo-responsive hydrogel. *Materials Horizons*, 4(4):694–700, 2017.

[Mohammad and Djurovic, 2016] Anees Mohammad and Sinisa Djurovic. Evaluation of fiber-optic sensing performance for embedded thermal monitoring of electric machinery wound components. In *Mediterranean Conf. on Embedded Computing*, pages 72–76, 6 2016.

[Munasinghe and Paul, 2019] Nuwan Munasinghe and Gavin Paul. Advanced Manufacturing of Spirals for Mineral Separation with Integrated Smart Sensing. In *IEEE UNITE*, 2019.

[Munasinghe and Paul, 2020a] Nuwan Munasinghe and Gavin Paul. Path Planning for Robot Based Radial Advanced Manufacturing Using Print Space Sampling. In *Int. Conf. on Control, Automation, Robotics and Vision*, 2020.

[Munasinghe and Paul, 2020b] Nuwan Munasinghe and Gavin Paul. Radial Slicing for Helical-Shaped Advanced Manufacturing Applications. *International Journal of Advanced Manufacturing Technology*, 2020.

[Munasinghe and Paul, 2020c] Nuwan Munasinghe and Gavin Paul. Ultrasonic-Based Sensor Fusion Approach to Measure Flow Rate in Partially Filled Pipes. *IEEE Sensors Journal*, 20(11):6083–6090, 2020.

[Munasinghe *et al.*, 2019a] M I N P Munasinghe, Lewis Miles, and Gavin Paul. Direct-Write Fabrication of Wear Profiling IoT Sensor for 3D Printed Industrial Equipment. In *Proceedings of the 36th Int. Symposium on Automation and Robotics in Construction (ISARC)*, pages 862–869, 2019.

[Munasinghe *et al.*, 2019b] Nuwan Munasinghe, Matthew Woods, Lewis Miles, and Gavin Paul. 3-D Printed Strain Sensor for Structural Health Monitoring. In *Int. Conf. CIS-RAM*, Bangkok, 2019. IEEE.

[Munasinghe *et al.*, 2021] Nuwan Munasinghe, John Masangkay, and Gavin Paul. Temperature Compensated 3D Printed Strain Sensor for Advanced Manufacturing Applications. In *IEEE Int. Conf. on Robotics and Automation*, 2021.

[Sauerbrunn *et al.*, 2015] Elizabeth Sauerbrunn, Ying Chen, Jeffrey Didion, Miao Yu, Elisabeth Smela, and Hugh A. Bruck. Thermal imaging using polymer nanocomposite temperature sensors. *Physica Status Solidi A*, 212(10):2239–2245, 10 2015.

[Shakor *et al.*, 2019] Pshtiwan Shakor, Shami Nejadi, Gavin Paul, and Sardar Malek. Review of Emerging Additive Manufacturing Technologies in 3D Printing of Cementitious Materials in the Construction Industry. *Frontiers in Built Environment*, 4(January), 2019.

[Tadjdeh, 2014] Yasmin Tadjdeh. 3D Printing Promises to Revolutionize Defense, Aerospace Industries. *National Defense*, 98(724):20–23, 3 2014.

[Traille *et al.*, 2011] Anya Traille, Sofiene Bouaziz, Stephane Pinon, Patrick Pons, Herve Aubert, Ali Boukabache, and Manos Tentzeris. A wireless passive RCS-based temperature sensor using liquid metal and microfluidics technologies. *European Microwave Week 2011: "Wave to the Future", EuMW 2011, Conference Proceedings - 41st European Microwave Conference, EuMC 2011*, (October):45–48, 2011.

[Wang *et al.*, 2019] Shicong Wang, Meisong Tong, Yangyang Guan, and Manos M. Tentzeris. 3D Printed Inverted-F Antenna and Temperature Sensor using Microfluidics Technologies. In *IEEE Int. Symposium on Antennas and Propagation and USNC-URSI Radio Science Meeting*, pages 599–600, 7 2019.

[Wickberg *et al.*, 2015] Andreas Wickberg, Jonathan B. Mueller, Yatin J. Mange, Joachim Fischer, Thomas Nann, and Martin Wegener. Three-dimensional micro-printing of temperature sensors based on up-conversion luminescence. *Applied Physics Letters*, 106(13), 2015.

[Wong and Hernandez, 2012] Kaufui V Wong and Aldo Hernandez. A Review of Additive Manufacturing. *ISRN Mechanical Engineering*, 2012(208760):10, 2012.

[Zhang *et al.*, 2014] Peng Zhang, Dongliang Cao, and Shaonan Cui. Resistivity-temperature behavior and morphology of low density polyethylene/graphite powder/graphene composites. *Polymer Composites*, 35(8):1453–1459, 8 2014.